

Instabilities of Obliquely Propagating Electromagnetic Modes in the Magnetosphere

G RENUKA & K S VISWANATHAN

Department of Physics, University of Kerala, Trivandrum 695 581

Received 26 April 1980 ; revised received 3 October 1980

The oblique propagation of the ordinary and the extraordinary electromagnetic modes in the magnetosphere and the instabilities in these modes arising from temperature anisotropy are studied. The dispersion equation is solved numerically using a TDC 316 computer for (i) McIlwain parameter $L = 2$ and 3 ; (ii) temperature anisotropy ratio $\delta (= T_{\perp}/T_{\parallel})$ values varying from 10 to 0.1 and (iii) for wavelength of waves of the order of a kilometre. The computer calculations are carried out for frequencies in the range ω_1 to $3\omega_1$ and ω_2 to $3\omega_2$, where ω_1 and ω_2 are the left-hand and right-hand cut-off frequencies, and both the real as well as the imaginary parts of the wave vector are calculated. It is found that both the ordinary and the extraordinary electromagnetic waves are unstable and the instability shows a strong dependence on the propagation angle θ , McIlwain parameter L , propagation frequency and also on the temperature anisotropy ratio δ .

1. Introduction

Instabilities of parallel propagating electromagnetic and electrostatic waves have been studied by several workers.¹⁻³ The wave normal angle of VLF emissions was observed by OGO-5 satellite and it was found that the chorus was often non-ducted and was thus propagating obliquely to the geomagnetic field.⁴ The linear stability analysis of obliquely propagating whistlers has been considered by Kennel.⁵

Brinca⁶ has analyzed the growth rate for oblique propagation in a cold plasma permeated by hot electrons and has shown that the growth rate does not necessarily become a maximum for propagation along the static magnetic field in comparison with propagation at an arbitrary wave normal direction. Taylor and Shawhan⁷ have dealt with the instability of Cerenkov radiation which is known to be mainly radiated in the direction close to the resonance cone angle. Hashimoto and Kimura⁸ have dealt with the problem of oblique propagation choosing a bi-maxwellian distribution function of hot electrons permeating a cold plasma.

The propagation of whistlers and other electromagnetic modes propagating parallel to the direction of the magnetic field is well understood, but there has been very little work on the nature of propagation and instabilities of the various kinds of electromagnetic modes propagating obliquely to the magnetic field. In this paper, we have presented the

studies of the instabilities of the obliquely propagating electromagnetic modes arising from temperature anisotropy in the distribution function.

2. Dielectric Permittivity Tensor of Plasma in a Magnetic Field

The dielectric permittivity tensor of a plasma in a magnetic field is given by the well known expression

$$\epsilon_{ij}(\mathbf{k}, \omega) = \delta_{ij} + 4\pi \sum_{\alpha} X_{ij}^{\alpha}(\mathbf{k}, \omega) \quad \dots(1)$$

where the components of the polarizability tensor X_{ij} and the explanation of the other parameters are given by Akhiezer *et al.*⁹

We shall assume that the electrons obey a distribution of the form

$$F = N_f \exp(-v_{\parallel}^2/u^2 - \mathbf{v}_{\perp}^2/w^2) \quad \dots(2)$$

where u and w are the thermal velocities and N_f is the normalization factor. This is an anisotropic velocity distribution function for the particles. Substituting for F one can easily verify, for the components of the polarizability tensor, the following results.

$$X_{11} = \frac{A \omega_c^2}{\omega^2 k_{\perp}^2} \sum_{l=-\infty}^{\infty} l^2 Q_l \psi_a \quad \dots(3)$$

$$X_{22} = \frac{A}{\omega^2} \sum_{l=-\infty}^{\infty} Q_3 \psi_a \quad \dots(4)$$

$$X_{33} = \frac{A}{\omega^2} \sum_{l=-\infty}^{\infty} Q_1 \psi_b - \omega_p^2 / (4\pi\omega^2) \quad \dots(5)$$

$$X_{12} = \frac{-iA\omega_c}{\omega^2 k_{\perp}} \sum_{l=-\infty}^{\infty} l Q_3 \psi_a \quad \dots(6)$$

$$X_{13} = \frac{A\omega_c}{\omega^2 k_{\perp}} \sum_{l=-\infty}^{\infty} l Q_1 \psi_c \quad \dots(7)$$

$$X_{23} = \frac{iA}{\omega^2} \sum_{l=-\infty}^{\infty} Q_2 \psi_c \quad \dots(8)$$

where

$$A = \omega_p^2 (k_{\parallel} u \pi^{3/2} \omega^2)^{-1} \quad \dots(9)$$

$$Q_1 = \frac{\omega^2}{2} \exp(-y) I_l \quad \dots(10)$$

$$Q_2 = \frac{\omega^4 k_{\perp}}{4\omega_c} \exp(-y) (I_l' - I_l) \quad \dots(11)$$

$$Q_3 = \frac{\omega^4}{4} \exp(-y) \left[y (I_l + I_l') + \left(1 - \frac{y}{2}\right) I_l' \right] \quad \dots(12)$$

$$\psi_a = i\pi \omega w^{-2} W(v_e/u) + k_{\parallel} x_5 y_1 \quad \dots(13)$$

$$\psi_b = y_1 \omega v_e w^{-2} + k_{\parallel} x_5 (0.5 \pi^{1/2} u^3 + v_e^2 y_1) \dots(14)$$

$$\psi_c = y_1 \omega w^{-2} + k_{\parallel} x_5 y_1 v_e \quad \dots(15)$$

where I_l is the modified Bessel function, $W(v_e/u)$ is the error integral and the argument of I_l is $k_{\perp}^2 w^2 / 2\omega_c^2$. Also,

$$y = k_{\perp}^2 w^2 / 2\omega_c^2 \quad \dots(16)$$

$$y_1 = u \pi^{1/2} + i\pi v_e W(v_e/u) \quad \dots(17)$$

$$x_5 = 1/u^2 - 1/w^2 \quad \dots(18)$$

$$I_l' = \frac{1}{2} [I_{l-1} + I_{l+1}] \quad \dots(19)$$

and

$$I_l'' = \frac{1}{4} [I_{l-2} + 2I_l + I_{l+2}] \quad \dots(20)$$

To study convective instability, we shall assume that ω is real whereas k is complex and let us write

$$k = k_r + i k_i \quad \dots(21)$$

The real and imaginary parts of the components of the dielectric permittivity tensor of the plasma in a magnetic field are then given by

$$\epsilon_{11}^R = 1 + \alpha^R [\beta_1 \cos \mu_i - \beta_2 \sin \mu_i] \quad \dots(22)$$

$$\epsilon_{11}^I = -\alpha^R \{\beta_2 \cos \mu_i + \beta_1 \sin \mu_i\} \quad \dots(23)$$

$$\epsilon_{22}^R = 1 + \alpha^R \{\beta_3 \cos \mu_i - \beta_4 \sin \mu_i\} \quad \dots(24)$$

$$\epsilon_{22}^I = -\alpha^R \{\beta_4 \cos \mu_i + \beta_3 \sin \mu_i\} \quad \dots(25)$$

$$\epsilon_{33}^R = 1 - \omega_p^2 \omega^{-2} + \alpha_1 \{\beta_5 \cos \mu_i - \beta_6 \sin \mu_i\} \dots(26)$$

$$\epsilon_{33}^I = -\alpha_1 \{\beta_6 \cos \mu_i + \beta_5 \sin \mu_i\} \quad \dots(27)$$

$$\epsilon_{12}^R = -\alpha_2 \{\beta_7 \cos \mu_i + \beta_8 \sin \mu_i\} \quad \dots(28)$$

$$\epsilon_{12}^I = -\alpha_2 \{\beta_8 \cos \mu_i - \beta_7 \sin \mu_i\} \quad \dots(29)$$

$$\epsilon_{13}^R = -\alpha_3 \{\beta_9 \cos \mu_i + \beta_{10} \sin \mu_i\} \quad \dots(30)$$

$$\epsilon_{13}^I = -\alpha_3 \{\beta_{10} \cos \mu_i - \beta_9 \sin \mu_i\} \quad \dots(31)$$

$$\epsilon_{23}^R = \epsilon_{23}^I = 0 \quad \dots(32)$$

where

$$\alpha^R = \omega_p^2 \omega^{-2} w^2 \exp(-\mu_r) \quad \dots(33)$$

$$\mu_r = k_{\perp}^2 w^2 \sin^2 \theta / 2\omega_c^2 \quad \dots(34)$$

$$\mu_i = 2k_i k_r w^2 \sin^2 \theta / 2\omega_c^2 \quad \dots(35)$$

$$\beta_1 = x_5 (x_6 + \pi^{1/2} \mu_i) + \frac{\pi^{1/2} \omega^2 \mu_i}{w^2 (\omega^2 - 4\omega_c^2)} \quad \dots(36)$$

$$\beta_2 = x_5 (x_6 \pi^{1/2} - \mu_i) + \pi^{1/2} \omega^2 w^{-2} \left[\frac{1}{\omega^2 - \omega_c^2} + \frac{\mu_r}{\omega^2 - 4\omega_c^2} \right] \quad \dots(37)$$

$$\beta_3 = x_5 (x_7 + \pi^{1/2} x_8) + \pi^{1/2} \omega^2 w^{-2} \{ \mu_i x_1 - (\mu^2)_i x_2 \} \quad \dots(38)$$

$$\beta_4 = x_5 (x_7 \pi^{1/2} - x_8) + \pi^{1/2} \omega^2 w^{-2} \left[\frac{1}{\omega^2 - \omega_c^2} + \mu_r x_1 - (\mu^2)_r x_2 \right] \quad \dots(39)$$

$$\beta_5 = x_3 x_7 + x_4 x_8 + \frac{x_5 \omega_c^2}{\cos^2 \theta} \left[(\mu_r + (\mu^2)_r) x_9 + (\mu_i - (\mu^2)_i) x_{10} \right] \quad \dots(40)$$

$$\beta_6 = x_4 x_7 - x_3 x_8 + \frac{x_5 \omega_c^2}{\cos^2 \theta} \left[(\mu_r + (\mu^2)_r) x_{10} - (\mu_i + (\mu^2)_i) x_9 \right] \quad \dots(41)$$

$$\beta_7 = \frac{[1 - \mu_r + \frac{3}{4}(\mu^2)_r]}{\omega^2 - \omega_c^2} + \frac{\{2\mu_r - (\mu^2)_r\}}{\omega^2 - 4\omega_c^2} + \frac{9}{8} \frac{(\mu^2)_r}{\omega^2 - 9\omega_c^2} \quad \dots(42)$$

$$\beta_8 = \frac{[\frac{3}{8}(\mu^2)_i - \mu_i]}{\omega^2 - \omega_c^2} + \frac{2\mu_i - (\mu^2)_i}{\omega^2 - 4\omega_c^2} + \frac{9}{8} \frac{(\mu^2)_i}{\omega^2 - 9\omega_c^2} \quad \dots(43)$$

$$\beta_9 = x_6 + \pi^{1/2} \mu_i \quad \dots(44)$$

$$\beta_{10} = \mu_i - x_6 \pi^{1/2} \quad \dots(45)$$

$$\alpha_1 = 2\omega_p^2 \omega^{-2} \exp(-\mu_r) \quad \dots(46)$$

$$\alpha_2 = \omega_p^2 \omega^{-1} \pi^{1/2} \omega_c \exp(-\mu_r) \quad \dots(47)$$

$$\alpha_3 = \alpha^R x_5 \tan \theta \quad \dots(48)$$

$$(\mu^2)_r = k_r^4 w^4 \sin^4 \theta / 4\omega_p^4 \quad \dots(49)$$

$$(\mu^2)_i = k_i k_r^3 w^4 \sin^4 \theta / \omega_p^4 \quad \dots(50)$$

$$x_1 = \frac{2}{\omega^2} - \frac{2}{\omega^2 - \omega_c^2} + \frac{1}{\omega^2 - 4\omega_c^2} \quad \dots(51)$$

$$x_2 = \frac{1}{\omega^2} - \frac{17/8}{\omega^2 - \omega_c^2} + \frac{1}{\omega^2 - 4\omega_c^2} - \frac{3/8}{\omega^2 - 9\omega_c^2} \quad \dots(52)$$

$$x_3 = 0.5(1 - u^2/w^2) + \frac{x_5 x_9 \omega^2}{u^2 \cos^2 \theta} \quad \dots(53)$$

$$x_4 = \frac{x_5 x_{10} \omega^2}{u^2 \cos^2 \theta} \quad \dots(54)$$

and

$$x_6 = 1 + \mu_r \quad \dots(55)$$

$$x_7 = 1 + \mu_r + \frac{(\mu^2)_r}{2} \quad \dots(56)$$

$$x_8 = \mu_i + \frac{(\mu^2)_i}{2} \quad \dots(57)$$

$$x_9 = k_r^2 - 2k_i k_r \pi^{1/2} \quad \dots(58)$$

$$x_{10} = k_r^2 \pi^{1/2} + 2k_i k_r \quad \dots(59)$$

It is evident from Eqs. (22)-(32) that the components of the dielectric permittivity tensor are dependent on the parallel and perpendicular temperatures. If n denotes the refractive index, the dispersion relation becomes⁹

$$A_1 n^4 + B_1 n^2 + C_1 = 0 \quad \dots(60)$$

where

$$A_1 = a_r + ia_i \quad \dots(61)$$

$$B_1 = b_r + ib_i \quad \dots(62)$$

$$C_1 = c_r + ic_i \quad \dots(63)$$

and a_r, a_i, b_r, b_i, c_r and c_i are given in terms of ϵ_{ij} and θ . Solving Eq. (60) we get k_i and k_r and hence we can study the growth and decay of the wave.

3. Numerical Results and Discussion

It is well known that for frequencies exceeding the electron plasma frequency, two types of electromagnetic modes exist: the ordinary and the extraordinary modes. The dispersion equation for these modes have been given by Cap¹⁰ for a cold

magnetized plasma. In this case, the minimum value of the frequency for the ordinary mode is the electron plasma frequency, whereas for the extraordinary mode, the minimum value is the right-hand cut-off frequency. The left-hand and right-hand cut-off frequencies are defined, respectively, as

$$\omega_1 = 0.5 \omega_c [(1 + 4\omega_p^2/\omega_c^2)^{1/2} - 1] \quad \dots(64)$$

and

$$\omega_2 = 0.5 \omega_c [(1 + 4\omega_p^2/\omega_c^2)^{1/2} + 1] \quad \dots(65)$$

We have studied the growth rates of the ordinary as well as extraordinary mode as a function of the temperature anisotropy parameters for different values of L, θ and other variables as shown below.

McIlwain parameter $L = 2$ and 3

Angle of propagation $\theta = 55^\circ$ to 65°

Temperature anisotropy $\delta = 10$ to 0.1

Frequency ratio ω/ω_1 , or $\omega/\omega_2 = 0.2$ to 2.8

Results of the numerical computations done using TDC 316 computer are shown in Figs. 1 to 5. The dependence of the growth rate, k_i (cm^{-1}), as a function of the frequency ratio ($\omega/\omega_1 = r_1$) for different values of the McIlwain parameter is depicted in Fig. 1. For $L = 2$, the ordinary mode first shows increase with increasing value of r_1 up to 1.8 and

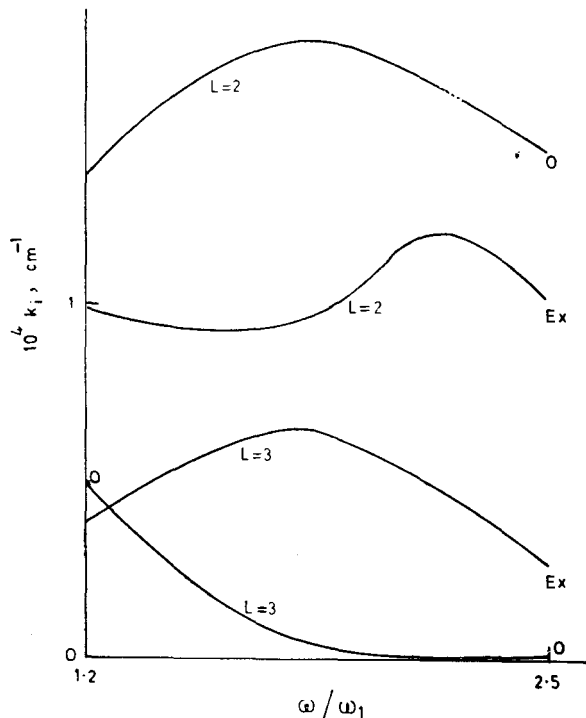


Fig. 1—Plots of growth rate k_i versus r_i for ordinary (O) and extraordinary (Ex) mode for $\delta = 10$ and $\theta = 60^\circ$

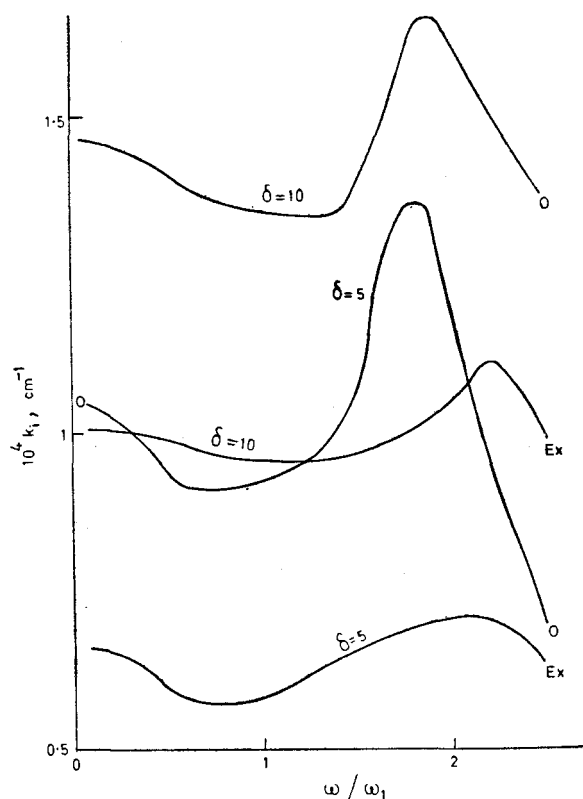


Fig. 2—Plots of k_i versus r_1 for $L = 2$, $\theta = 55^\circ$, $\delta = 10$ and 5 for ordinary (O) and extraordinary (Ex) modes

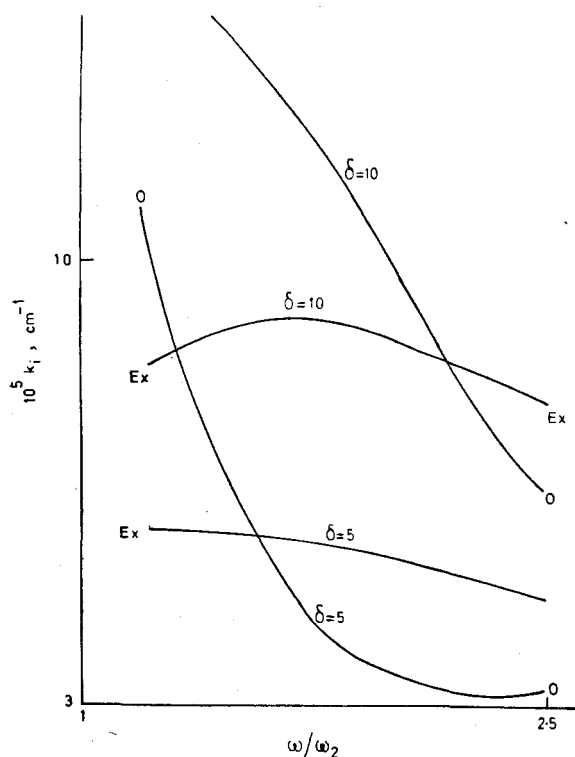


Fig. 3—Plots of k_i versus r_2 for $L = 2$, $\theta = 55^\circ$, $\delta = 10$ and 5 for ordinary (O) and extraordinary (Ex) modes

then decreases, whereas for the extraordinary mode the wave shows oscillating nature with increase of r_1 values. But for $L=3$, the growth rate decreases with increasing r_1 for the ordinary mode whereas it shows a maximum for extraordinary mode, increasing initially up to $r_1 = 1.8$ and thereafter steadily decreasing.

The frequency dependence of growth rate of the wave can be seen from Figs. 2 and 3. The nature of wave growth for $\theta=55^\circ$, $\delta=5$ and 10 at $L=2$ as a function of r_1 is plotted in Fig. 2. In Fig. 3 is shown the growth rate for frequencies exceeding the right-hand cut-off frequency for different values of the anisotropy parameter δ . In this case, the growth rate values are about 20 times greater than that for r_1 variation case.

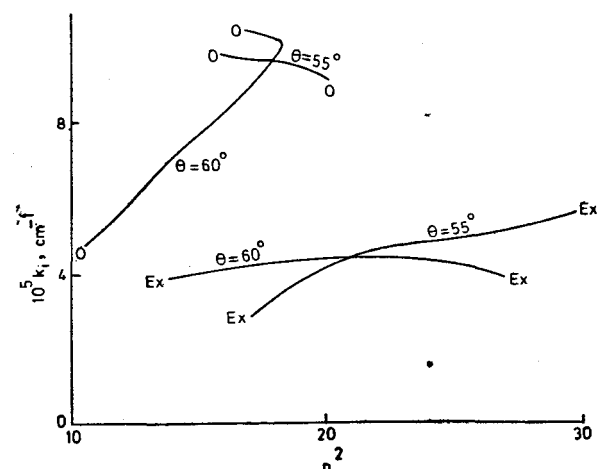


Fig. 4—Plots of k_i versus n^2 for $L = 3$, $r_1 = 1.2$, $\theta = 55^\circ$ and 60° for ordinary (O) and extraordinary (Ex) modes

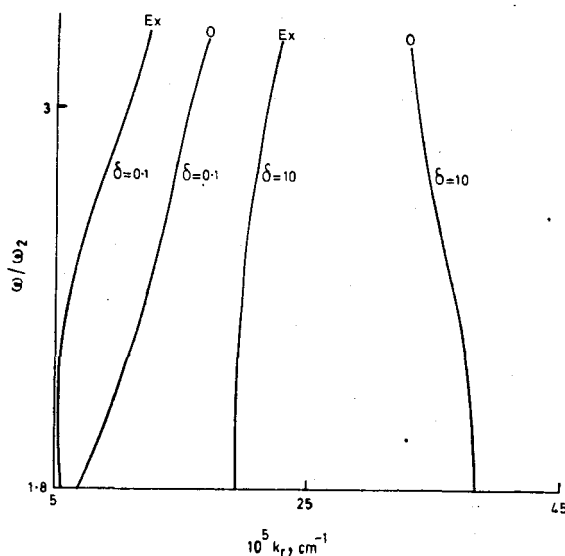


Fig. 5—Plots of r_2 versus k_r for $L = 2$, $\theta = 60^\circ$, $\delta = 0.1$ and 10 for ordinary (O) and extraordinary (Ex) modes

Fig. 4 shows the growth rate with n^2 for the waves at $L = 3$, $r_1 = 1.2$ and $\theta = 55^\circ$ and 60° .

The real part of the growth rate k_r is plotted against $r_2 (= \omega/\omega_2)$ in Fig. 5 for the values of $\delta = 0.1$ and 10 at $L = 2$ and $\theta = 60^\circ$. The curves look like a series of vertical lines perpendicular to the k_r axis. For a given r_2 , k_r is larger for larger values of δ or the wavelength decreases with increasing values of δ .

References

48

1. Kennel C F & Petschek H E, *J. geophys. Res.*, 71 (1966), 1.
 2. Lee K F, *J. plasma Phys.*, 6 (1971), 449.

3. Ashour-Abdalla M, Chanteur G & Pellat R, *J. geophys. Res.*, 80 (1975), 2775.
 4. Thorne R M, Smith E J, Burton R K & Holtzer R E, *J. geophys. Res.*, 78 (1973), 1581.
 5. Kennel C F, *Phys. Fluids*, 9 (1966), 2190.
 6. Brinca A L, *J. geophys. Res.*, 77 (1972), 3495.
 7. Taylor W W L & Shawhan S D, *J. geophys. Res.*, 79 (1974), 105.
 8. Hashimoto K & Kimura I, *J. plasma Phys.*, 18 (1977), 1.
 9. Akhiezer A I, Akhiezer I A, Polovin R V, Sitenko A G & Stepanov K N, *Collective oscillation in a plasma* (Pergamon Press, New York), 1967.
 10. Cap F F, *Handbook on plasma instabilities, Vol. 1* (Academic Press, New York), 1976.